TRAJECTORY GENERATION OR INPUT SHAPING?

Input shaping can effectively reduce residual vibrations in flexible systems induced by the position trajectory. But misunderstanding of the implementation aspects and its use has led to limited applications in mechatronic systems, where the shaped reference trajectory could result in a reduced overall movement time. The main contribution of this article is a design method based on the relationship of the relative overshoot with the ratio of vibration time and move time. This allows the determination of the highest acceleration value that keeps accuracy within the desired range.

ROBBERT VAN DER KRUK AND AREND-JAN VAN NOORDEN

Introduction

Unwanted residual vibrations often limit the productivity of product handling by vacuum grippers or other suspended means. The pick & place actions in robotic systems often contribute the most to the vibration of the products to be handled. Input shaping provides a way to suppress the residual vibration frequency from the reference by shaping the spectral content of the motion profile by means of time-delay filters. Singer and Seering [1] created the framework of input shapers in the nineties.

For the control of cranes, the usefulness of input shaping is well known and implemented. However, a big knowledge gap is noted for applying input shaping to robotic systems. When robots have to operate in unknown environments, it is not sufficient to plan beforehand. They need to react to their sensors. In that case, a trajectory needs to be generated to execute the task within constraints such as maximum speed and acceleration, interpolating between waypoints to provide the reference position trajectory in real time. Trajectories for moving in a single direction, with constrained acceleration, are shown in Figure 1. We ignore the constant-velocity part of the trajectory, as it has limited effect on the dynamics and is not even reached for fast pick & place moves.

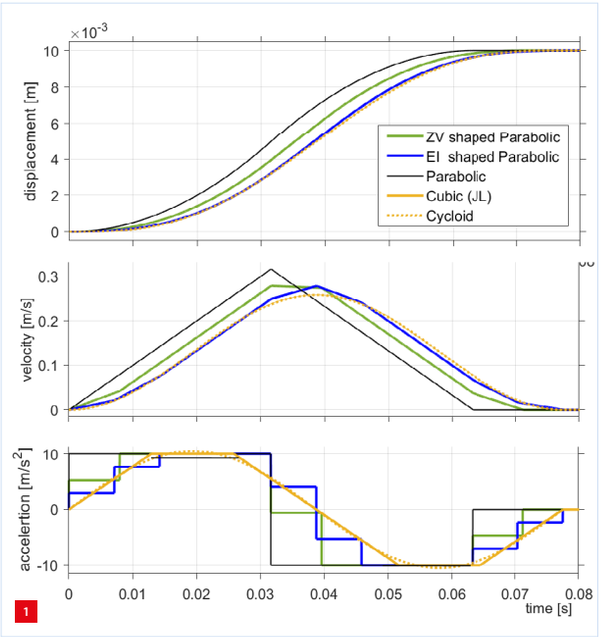

1

Acceleration-constrained comparison of parabolic, cubic, cycloid and ZV- and EI-input-shaped parabolic trajectories. ZV and EI stand for Zero Vibration and Extra Insensitive, respectively; see the text for explanation.

The topic of trajectory generation is related to the study of cam-shaft profiles [2], where cycloid profiles are widely used. Wim van der Hoek [3] introduced the $u_0(\tau)$ diagrams to clarify the relation between the relative overshoot u_0 and the relative vibration time τ. The objective was the design of lightweight and very stiff mechanisms in order to achieve high positional accuracy at high speeds.

Using Van der Hoek's notation, we define:

$$u_0 = \frac{\max|r - x(t)|}{r}, \quad t > T_m \tag{1}$$

$$\tau = \frac{T_d}{T_m} \tag{2}$$

Here, $x(t)$ is the position of the object, r is the reference end position, T_d is the damped vibration time and T_m is the shaped reference move time.

In this paper, we use the $u_0(\tau)$ diagrams to relate overshoot to relative move time for selecting input-shaper methods and maximum acceleration. Trajectory profiles are commonly expressed in polynomials of second or higher order. It is usually concluded that their limited third derivative, or jerk, results in an attractive response as it approaches the cycloid; see Figure 1. However, the parabolic profile features the shortest move time. The parabolic

AUTHORS' NOTE

During the research described in this article, Robbert van der Kruk was a senior academic researcher in the Control Systems Technology group at Eindhoven University of Technology (TU/e) in Eindhoven (NL). He is a former R&D manager at Philips, ASML and Agilent Technologies. Arend-Jan van Noorden is a mechatronics engineer at ASML in Veldhoven (NL).

r.j.v.d.kruk@tue.nl
www.tue.nl/cst

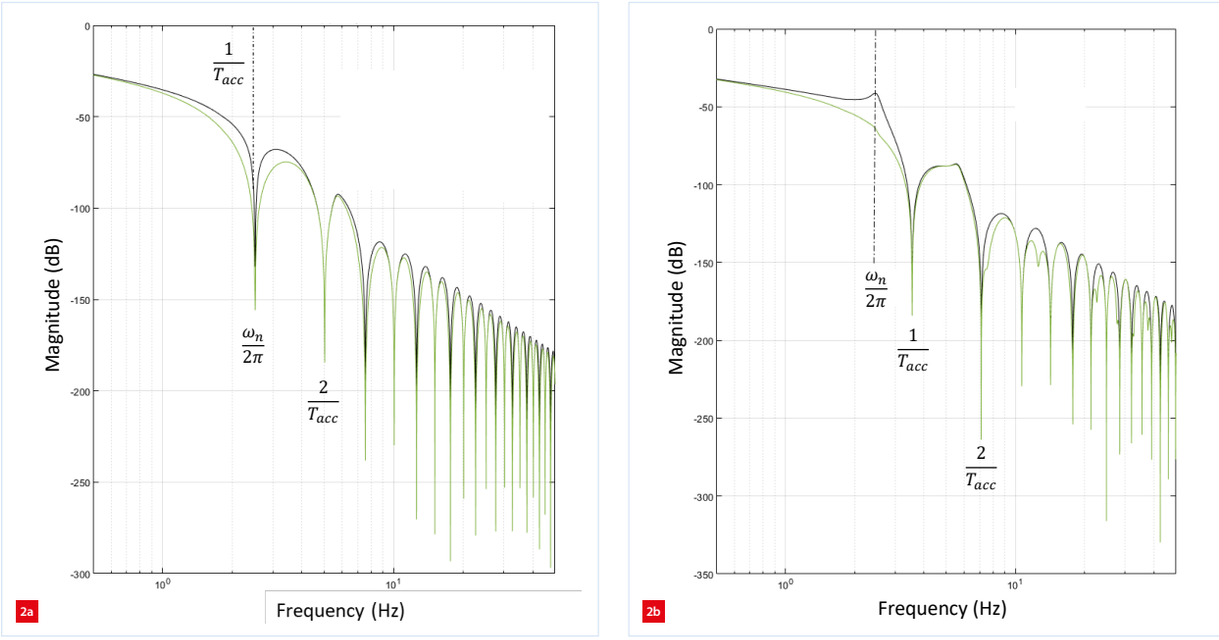

Frequency responses of a robotically suctioned object excited by a parabolic (black) and ZV-input-shaped parabolic (green) trajectory, respectively. (a) τ = 0.5. (b) τ = 0.7.

and cubic, or Jerk-Limited (JL), trajectory profiles are available in most industrial digital motion controllers. The frequency response of the output x of the system excited by a (ZV-input-shaped) parabolic trajectory consists of sync pulses; see Figure 2 for an example.

The framework of input shapers was created in the time domain. For educational purposes, we will review input shapers and trajectory generation in both the time and the frequency domain (a detailed analysis is given in [4]). Typically, the main system excitation is not external but is generated by the trajectory itself. Some residual vibrations may exceed the error bounds and, therefore, affect the overshoot and settling performance. Figure 2 depicts the frequency spectrum of a flexible system excited by an unshaped and a shaped parabolic trajectory.

Input-shaping methods use superposition of delayed parts of the original profile such that the steady-state position equals the original end position. The residual vibration is suppressed by generating an input that cancels its own vibration. The simplest input shaper, the ZV (Zero Vibration) shaper, provides zero vibration at the desired frequency and consists of two impulses. The first impulse starts the system vibrating, the second impulse is delayed by a half period of the damped vibration, thereby cancelling it. The two parameters of the ZV shaper are the damped vibration period T_d and the damping ratio ζ.

The Extra Insensitive (EI) method [1] uses an additional branch (a third pulse trailing the existing two ZV pulses) with a full delay of T_d. Unlike the ZV shaper, it does not attempt to force the vibration to zero. A small level of vibration is allowed at the modelling frequency, while enhancing the insensitivity to frequency modelling errors. The ZV shaper and its derivative(s) are made using a constraint that there should be zero vibrations at the desired frequency. The constraints of the shaper could be relaxed such that its residual vibration percentage remains below a tolerable vibration level specified by the designer. The EI shaper utilises this idea. The main advantage of relaxing these constraints is that a higher robustness can be achieved with the same time elongation of the shaped trajectory as with the ZVD (Zero Vibration Derivative) shaper. The large insensitivity of high-order EI shapers is rarely needed. The three parameters of the EI shaper are T_d, ζ and tolerable vibration level.

The jerk-limiting input shaper (JL) can be created by a Finite Impulse Response (FIR) filter applied to the parabolic trajectory or by direct generation of a trajectory. The JL shaper has only one parameter, the desired damped vibration period. The difference equations of these input shapers are given in [4].
Input shaping of the parabolic reference results in pulsed acceleration profiles for ZV and EI as shown in Figure 1. Notice here the difference with the smooth acceleration profile of the cycloid and the cubic profile. Input shaping of the trajectory is realised by a simple digital filter and can be used to process the acceleration, velocity or position data such that the implementation is independent of trajectory generation and control algorithms.

The frequency responses (Bode diagrams) of the input shapers are plotted in Figure 3. The magnitude plot shows

stop bands around the natural frequency $1/T_d$; the damped natural vibration is suppressed. The EI shaper has the widest stop band at the price of a time elongation T_d as demonstrated in Table 1. The negative shapers as reported by [5] reduce the move time significantly. However, their disadvantage is the excitation of high-frequency modes and the lack of guarantees for the shaped input signal. They cannot be used reliably. Conventionally designed frequency-domain filters such as notch and low-pass filters are never better than the mentioned input shapers, as proven in [6].

Table 1
Input-shaped reference trajectories and their move times and relative vibration times.

Trajectory and input shaper	T_m	τ
Parabolic	$2T_{acc}$	$T_d / (2T_{acc})$
Parabolic & ZV	$2T_{acc} + T_d/2$	$T_d / (2T_{acc} + T_d/2)$
Parabolic & EI or JL	$2T_{acc} + T_d$	$T_d / (2T_{acc} + T_d)$

T_d = damped natural vibration time.

T_{acc} = acceleration time of the parabolic profile.

Performance criteria for pick & place motions

The unwanted vibrations are typically excited if the spectral content of the trajectory profile overlaps with the resonance frequencies of the mechanism. As input shaping leads to elongation of the motion profile, we include this in the move time, see Table 1. The importance of the $u_0(\tau)$ relation is that for a prescribed displacement, overshoot and given vibration time, a maximum value of τ is found, resulting in a minimum move time of the trajectory.

Additionally, Figure 2 shows the influence of τ in the frequency response. In [7], it is concluded that the combined input-shaper and PD-feedback control results in superior controllers for one-mass-spring-damper systems

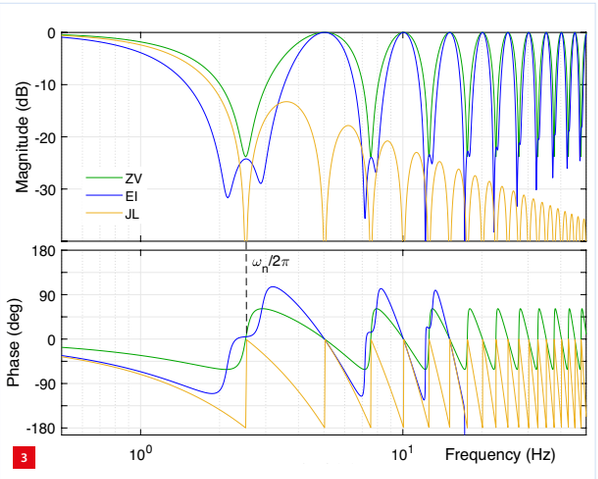

Frequency responses of the input shapers.

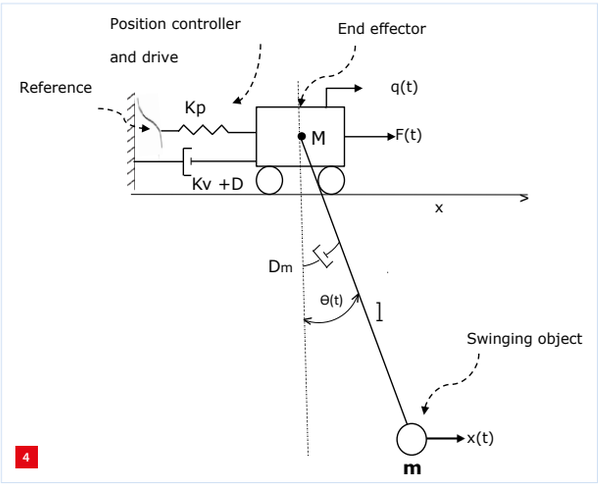

Abstraction of the handling of a swinging product picked by a suction cup: a suspended pendulum driven by a position-controlled cart.

when the design constraints do not force an overdamped system. The input shapers reduce the overshoot towards zero, while the feedback controller reduces the non-linearities, disturbances and modelling errors. The $u_0(\tau)$ relations will be derived in the next section, to reach conclusions on the superiority hypothesis of the combined PD-feedback control and input shaper for robotic systems handling swinging products.

Robotic pick & place of swinging products

The robot mechanism is considered as a rigid body; the bandwidth of the joint controllers is significantly higher than the resonance frequency of the product, while the lowest resonance frequency of the mechanical system is typically much higher than the controller bandwidth. Robotic packaging requires fast pick & place cycles of suspended food packages. When suction cups are used, the product turns into a swinging load when moved. For a physical model of the robot manipulator and the product, we consider the robot end-effector as a position-controlled cart that moves in the horizontal direction and a load that swings in the vertical plane. The horizontal movement $x(t)$ of the load is observed and expected to meet the positional requirement; see Figure 4.

The equations of motion of the horizontal movement of the object (m) are based on a pendulum driven by the mass M, as depicted in Figure 4, with two independent coordinates q and θ. The horizontal movement of m depends on these two coordinates according to (6). The position-controlled motion of the cart is modelled by a spring K_p and a damper K_v to model a digital PD controller. The bandwidth ω_c and relative damping β_c of the position-controlled cart are:

$$\omega_c = \sqrt{\frac{K_p}{(M+m)}}, \quad \beta_c = \frac{K_v}{2\sqrt{K_p(M+m)}} \qquad (3)$$

The Lagrange equations lead to the differential equations of motion:

$$K_p(r-q) - (K_v + D)\dot{q} = (M+m)\ddot{q} + ml\ddot{\theta}\cos(\theta) - ml\dot{\theta}^2\sin(\theta) \quad (4)$$

$$ml\ddot{q}\cos(\theta) + ml^2\ddot{\theta} + D_m\dot{\theta} + mlg\sin(\theta) = 0 \quad (5)$$

$$x = q + l\sin(\theta) \quad (6)$$

The natural frequency ω_n of the vibration of the product can be obtained from (4) by neglect of the damping D and D_m of the cart and mass, respectively, at small values of θ:

$$\omega_n = \sqrt{\frac{g(M+m)}{Ml}} \approx \sqrt{\frac{g}{l}} \quad (m \ll M) \quad (7)$$

It depends largely on l, the equivalent length of the product in the gripper. The control scheme in Figure 5 shows the position of the product, the controlled variable x, which is not directly measured but estimated from a secondary measurement q, i.e. the actuator positions, by shaft encoders. The joint feedback controllers C eliminate disturbances such as load changes and friction.

Initially, a sensor tag was attached to the product to be used for one-time measuring x and to shape the controller. The values T_d and ζ of the suspended product could be derived from the joint position error of the drive signal in the servo controllers. From (4), (5) and (6), simulations of the responses of the load position for parabolic and input-shaped parabolic trajectories were collected.

Typically, the joint controllers of the robot are shaped for a fast and accurate response with high servo stiffness of the end-effector, resulting in a bandwidth higher than the vibration frequency of the load. The frst term in (5) represents the inertial force transmitted to the pendulum mass m and is usually highest at the moment the acceleration switches to deceleration. To provide additional

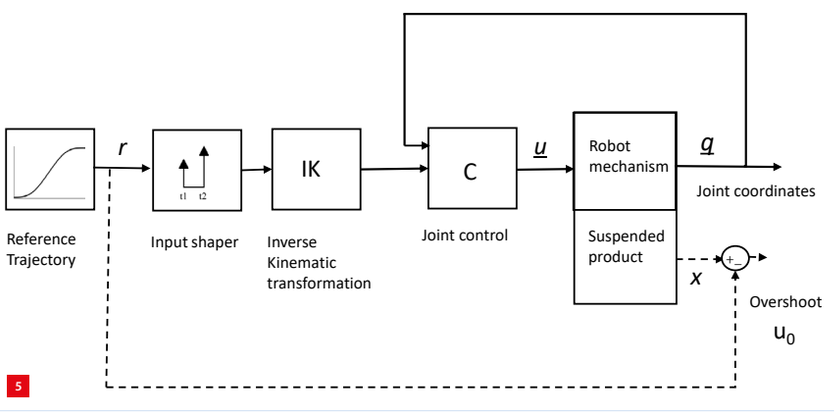

Robotic control structure with inferential control. The dashed line indicates that the performance output x is not measured during operation.

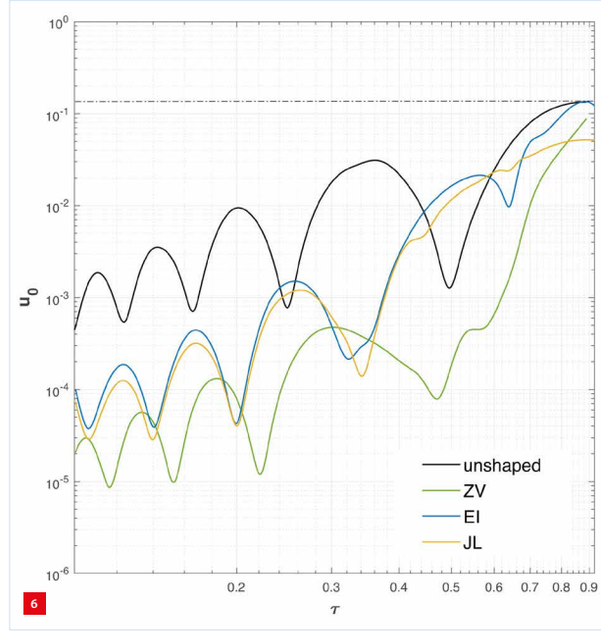

Simulation results for the cart-pendulum system: relative overshoot u_0 as a function of τ for shaped and unshaped parabolic trajectories. The damping offset (deviation from the model value) is 10%.

damping of the pendulum, we match the bandwidth of the controller to the frequency of vibration ($\omega_c = \omega_n$) with relative controller damping $\beta_c = 1$. As a result, the control parameters are reduced to:

$$K_p = \omega_n^2(M+m), \quad K_v = 2\omega_n(M+m). \quad (8)$$

The input shaper ZV combined with this impedance match is named ZV&IM.

Simulation results

The simulation results are depicted in Figure 6. The move time T_m is set to realise τ using the values in Table 1 with known vibration period T_d according to the scheme of Figure 7, demonstrating a design procedure for the parameters of the input shapers and the maximum acceleration of the parabolic trajectory. This maximum acceleration is not a constant and needs to be selected for 'no swing moves'.

At unit fractions of T_d/T_{acc}, where $\tau = 1/2, 1/4, 1/6, \ldots$, the overshoot of the pendulum approaches zero. Due to the strong inertial coupling, the swing excited during the acceleration period is exactly cancelled during the deceleration period. This behaviour was also described by [3, chapter 8].

In the range $\tau < 0.4$, all input shapers reduce the overshoot significantly. Here, the move time is much larger than the vibration time and only a low level of vibration is excited. In the interval $0.4 < \tau < 0.6$, the EI and JL input shapers do not contribute to overshoot reduction. For $\tau > 0.6$, the move time approaches the vibration period. The ZV input shapers

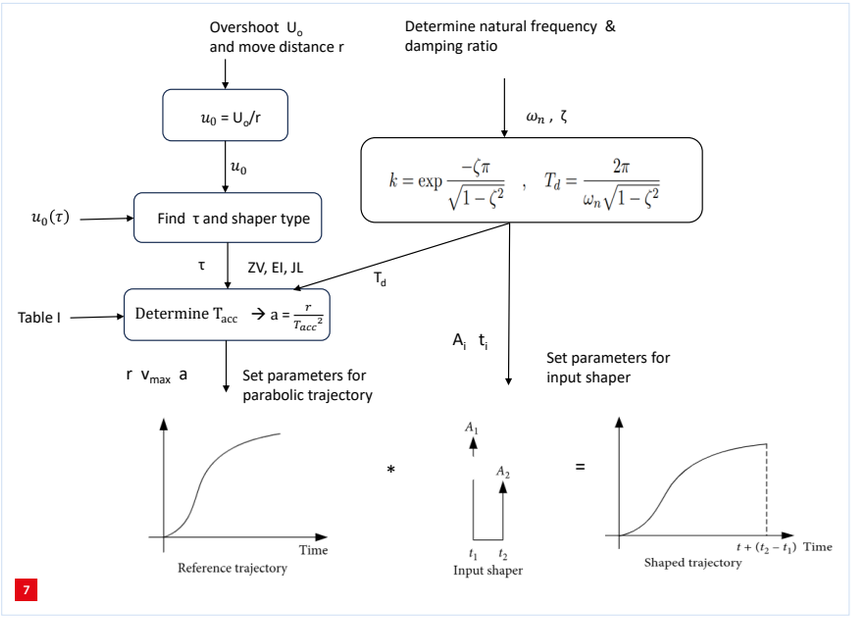

Design procedure for the trajectory generator input shaper.

reduce the overshoot significantly, with a factor of 10, for values of $\tau < 0.8$. The EI and JL input shapers reduce the overshoot as well, but not as strong as the ZV shaper. The responses of the input shapers ZV, JL and ZV&IM with equal move time ($\tau = 0.7$) are shown in Figure 8.

The unshaped response is hardly damped, which results in vibrations approaching the equivalent length of the product. Clearly, the ZV shaper has the highest overshoot reduction. The sensitivity of the relative overshoot to variations of the equivalent pendulum length l is plotted in Figure 9. The ZV shaper has the lowest overshoot when tuned well in case of small variations. Within the range of 10% length variations,

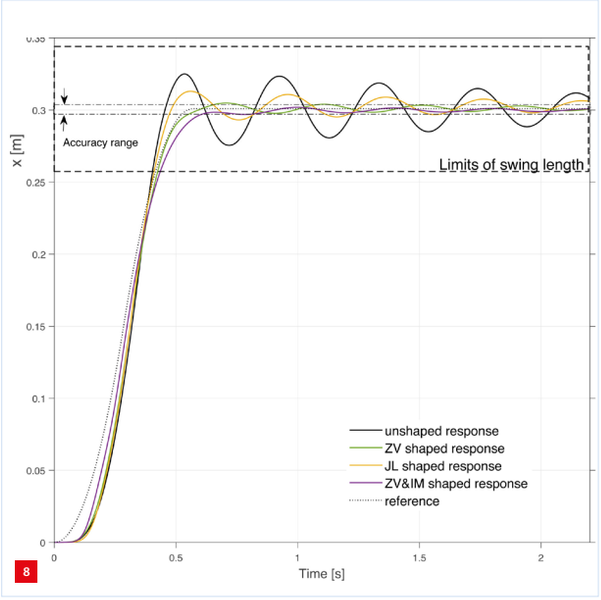

Displacement responses for parabolic shaped trajectories. Overshoot is 25.5 mm (unshaped), 9.4 mm (JL), 2.9 mm (ZV&IM) and 2.7 mm (ZV), respectively. The damping offset is 10%, at τ = 0.7.

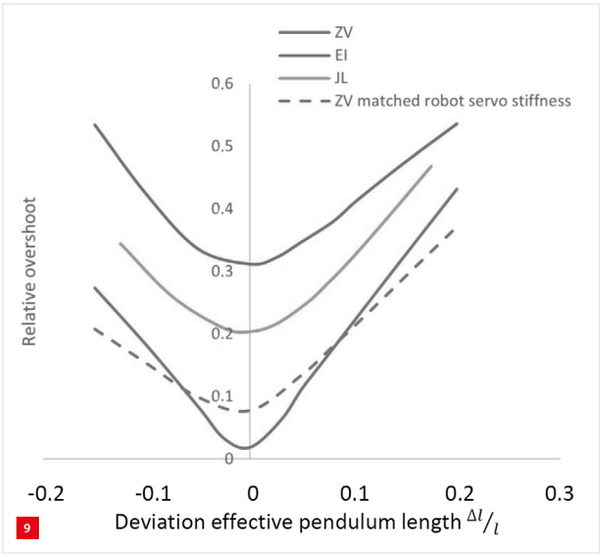

Sensitivity of the overshoot to variations of the equivalent pendulum length for ZV, EI, JL and ZV (with matched robot servo stiffness), at τ = 0.7.

the ZV shaper features the highest suppression. In the range of 10-20%, the ZV shaper performs best when the bandwidth of the robot servo controllers is matched to the vibration frequency of the swinging product. The EI shaper provides better insensitivity for even larger variations.

Experimental results

The high-volume industrial case packaging of sealed food is typically realised with fast delta robots of which the paths can be programmed to stack the products identified by a fixed camera at the entry of the conveyor belt. An example of a viscous product in a fluid bag is demonstrated in Figure 10. The throughput limitation of the point-to-point movements is caused by the peel-off and the oscillations during placement. Inaccurate placement or collision with the box by overshoot can result in damaged products or misplacement. Different travel times between axes can be equalised by delaying the axis taking the longest travel time or shaping all axes equally.

It has been shown in [8] that the vacuum-gripped products suspended by the end-effector behave dominantly as a pendulum. The product variations are limited to frequencies in the range of 2-2.8 Hz. To detect the displacement of the product, a visual fiducial system attached to the front of the bag is used, as shown in Figure 10. The 3D pick & place path is defined by four user-defined positions, P_0 to P_3. The straight lines are connected by blends (bent curves) to create a smooth path defined by B-splines. The 3D-task-oriented coordinate system uses the inverse kinematic transform to create the joint displacements every 1 ms. Input shaping is executed in task coordinates.

Figure 11 plots the experimental results (25 measurements) for parabolic and its ZV-shaped trajectories for horizontal

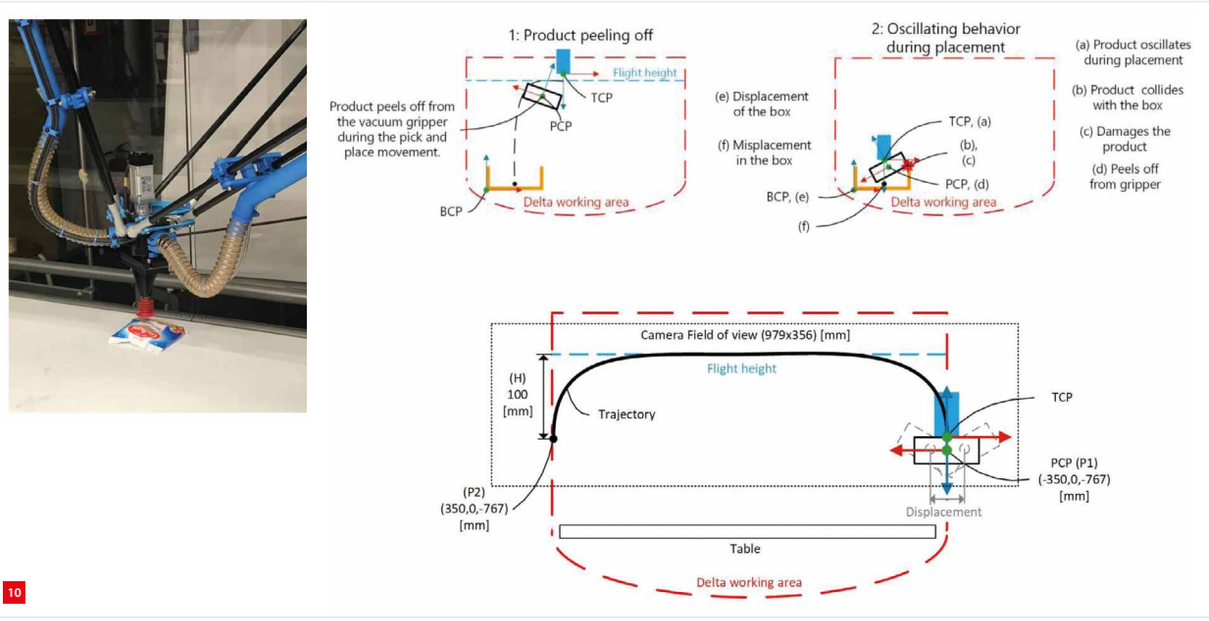

Swinging cheese bag picked by a delta robot with vacuum gripper (source: Blue Print Automation, Woerden (NL)). The view on the right shows the test path of the product-centre point (PCP); TCP is the tool-centre point.

and vertical directions. Note that the acceleration of the product-centre point (PCP) is reduced by almost a factor of two. To investigate the ZV-shaper performance in a production environment, a use case test was executed: the placement inside a box within an overshoot of less than 15 mm. A twofold decrease in travel time at the expense of slightly higher product accelerations was found when both *x*- and *z*-axes were input-shaped during motion.

To find the move time decrease until the product starts to peel off, a maximum horizontal PCP acceleration of 20 m/s^2 was imposed. This resulted in a 14% decrease in travel time and a vibration reduction of 32%. Synchronisation was needed to conserve the original spatial reference path.

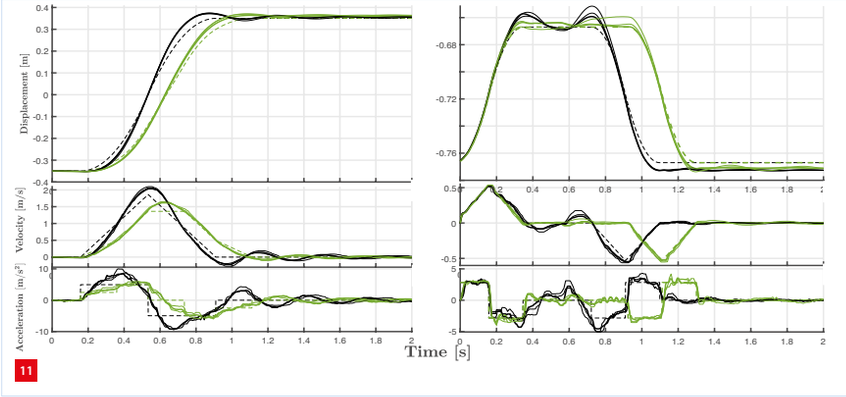

Measured displacement, velocity and acceleration of unshaped and shaped responses for tool-centre point (left) and product-centre point (right) in horizontal and vertical direction. For each quantity, three measurement curves have been plotted (maximum, minimum and modus response) at τ = 0.4.

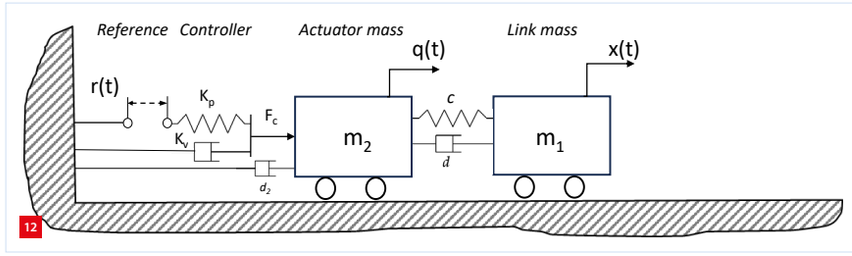

Two-mass-damper-spring model to represent the actuator axis coordinate q and link position x of a flexible-joint robotic mechanism. The actuator mass m_2 is driven by a PD controller with parameters K_p, K_v via a motor and a current amplifier such that the force is proportional to the output of the controller.

Pick & place with flexible-joint robots

In practice, robot mechanisms cannot be considered as rigid bodies and their dynamical behaviour is often dominated by the lowest frequency mode. Typically, a model with two masses connected by springs and dampers provides an effective model, as depicted in Figure 12.

The equations of motion are:

$$m_2\ddot{q} = K_p(r-q) - K_v\dot{q} - d_2\dot{q} - c(q-x) - d(\dot{q}-\dot{x}) \quad (9)$$

$$m_1\ddot{x} = c(q-x) + d(\dot{q}-\dot{x}) + F_d \quad (10)$$

The resonance and anti-resonance frequencies are:

$$\omega_r = \sqrt{\frac{c(m_1+m_2)}{m_1 m_2}} \quad \omega_a = \sqrt{\frac{c}{m_1}} \quad (11)$$

The closed-loop bandwidth ω_c is selected to minimise the position error of the link at the start of the dwell [9] at a servo damping ratio of 1.0:

$$\omega_c = 0.8\omega_a \quad K_p = (m_1+m_2)\omega_c^2 \quad K_v = (m_1+m_2)\omega_a \quad (12)$$

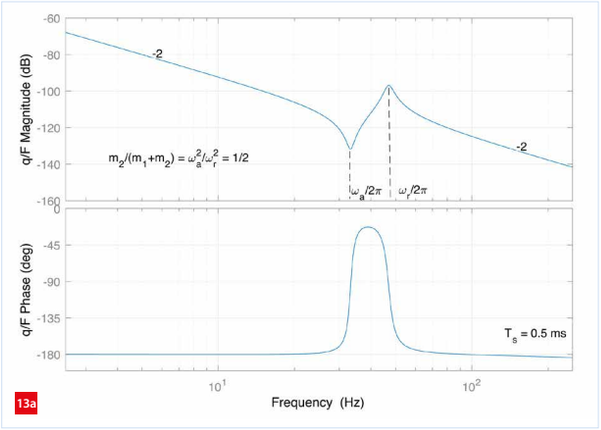

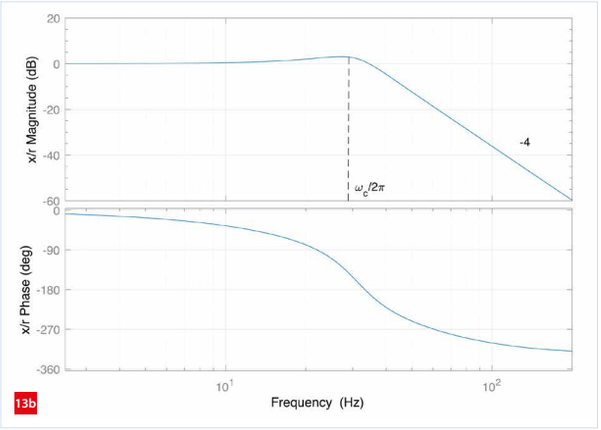

Control for a two-mass-spring-damper system.
(a) Open-loop joint transfer function.
(b) Closed-loop joint transfer function.

The frequency responses of the open-loop and controlled (closed-loop) system are depicted in Figure 13.

Simulation results

The simulation results are depicted in Figure 14, which corresponds to Figure 6 for the cart-pendulum-mass case. For $\tau < 0.2$, the move time is much longer than the natural vibration period and the system behaves similar to a rigid body. The $u_0(\tau)$ relation is quadratic. The EI, JL and ZV shapers result in, respectively, a 20-, 6- and 5-fold reduction of the overshoot as compared to the parabolic trajectory with equal move time. The EI shaper features the smallest overshoot compared to the other shapers with equal move time; this comes at the price of a slightly higher driving force.

This result is important for accurate applications that require minimum overshoot. Here, the application area is accurate positioning with a long move time, such as in portal coordinate measuring machines [10], electron microscopes and accurate 3D printing.

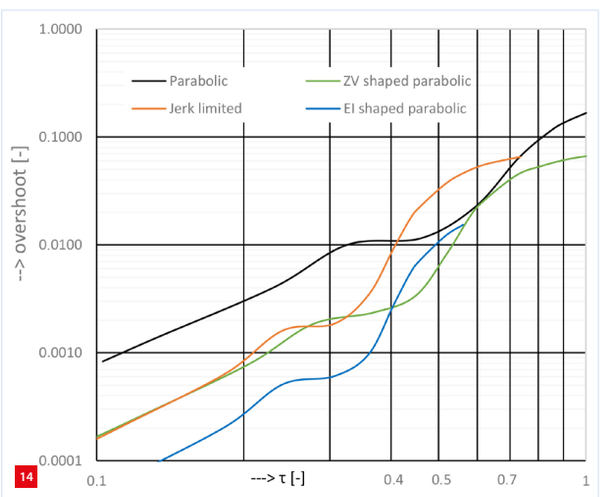

Two-mass-spring-damper system: relative overshoot u_0 as a function of τ for unshaped and ZV-, EI- and JL-shaped parabolic trajectories. The shaper frequency mismatch is 5%, the damping offset is 10%.

In the range $0.4 < \tau < 0.7$, input shaping has a lower contribution to reducing the vibration. The JL shaper even worsens the performance. For $\tau > 0.7$, the move time approaches the period of natural vibration; a significant reduction of the vibration can only be obtained with the ZV shaper. Note that in this range the overshoot of the parabolic trajectory exceeds 5%, which is often unacceptable.

The time responses with equal travel time $\tau = 0.75$ are depicted in Figure 15. The overshoot is reduced by 50%. State-of-the-art wire bonders for semiconductor devices should perform motions with horizontal strokes of one tenth of a millimeter up to several millimeters while exhibiting peak accelerations of more than 250 m/s^2. Such motions may excite machine dynamics and induce unwanted vibrations that hamper the quality of bonding. Experimental results with input shapers show a 70% variance reduction of the amplitude of the residual vibration ($\tau \approx 0.8$).

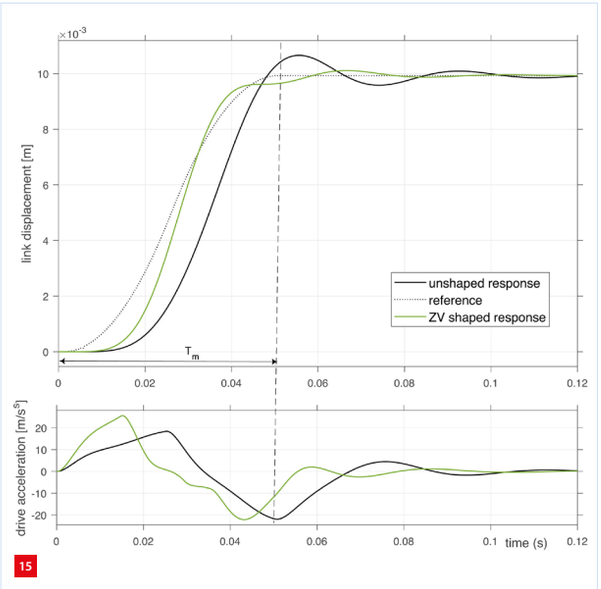

Simulation results for link position and drive acceleration response for the unshaped and the ZV-input-shaped trajectory, at τ = 0.75.

Conclusion

A method of control has been developed that eliminates the need for restricted accelerations for swing-free robotic product handling. This method uses fast input shapers to eliminate the natural vibration from the reference in the task space of the robot, such that the shortest acceleration/deceleration time is used for the reference trajectory.

The relative move time τ has a major influence on the overshoot with and without the use of input shapers. Relations of the relative overshoot as a function of τ for the relevant input shapers have been derived for robotic pick & place positioning of swinging products and for flexible-joint systems. This provides the backbone of a design procedure for the parameters of the input shapers and the allowable acceleration of the parabolic trajectory; these need to be selected for each critical point-to-point move.

For swinging products with length variations less than 10%, the ZV shaper features the largest vibration reduction. In the range of 10-20% variations, the ZV shaper performs best when the bandwidths of the axis motion controllers are matched to the vibration frequency of the swinging product.

For accurate applications with a long move time with flexible-joint robots that require minimum overshoot, the EI shaper is preferred. Jerk-limited reference trajectories can be regarded as input-shaped parabolic reference trajectories. Their performance is inferior to ZV shapers, but can effectively reduce the excitation of high-frequency modes.

A clear distinction should be made between trajectory generation to prevent saturation of the actuators only, to enable path synchronisation, and filtering of the trajectory for dynamic swing-free response, to obtain minimum move time and swing-free results. The trajectory, as such, is parameterised by displacement, move time and maximum acceleration only. Jerk and snap phases of the trajectory need to be avoided, as they create trajectories inferior to those achieved with the control method described in this article.

REFERENCES

[1] N.C. Singer, and W.P. Seering, "Preshaping Command Inputs to Reduce System Vibration", *Journal of Dynamic Systems, Measurement, and Control*, vol. 112 (1), pp. 76-82, 1990.

[2] H. Kwakernaak, and J. Smit, "Minimum vibration cam profiles", *Journal of Mechanical Engineering Science*, vol. 10 (3), pp. 219-227, 1968.

[3] W. van der Hoek, *Het voorspellen van het dynamisch gedrag en positioneernauwkeurigheid van constructies en mechanismen*, TU/e Department of Mechanical Engineering, 1984.

[4] R. van der Kruk, A.-J. van Noorden, T. Oomen, R. van de Molengraft, and H. Bruyninckx, "Robotic control for vibration reduction of swinging products", *2023 IEEE In ternational Conference on Mechatronics* (ICM), pp. 1-8, 2023.

[5] M. Lau, and L. Pao, "Comparison of input shaping and time-optimal control of flexible structures", *ACC*, vol. 2, pp. 1485-1490, 2001.

[6] W. Singhose, and J. Vaughan, "Reducing vibration by digital filtering and input shaping", *IEEE Transactions on Control Systems Technology*, vol. 19 (6), pp. 1410-1420, 2011.

[7] J.R. Huey, "The Intelligent Combination of Input Shaping and PID Feedback Control", Ph.D. thesis, Georgia Institute of Technology, 2006.

[8] A.-J. van Noorden, "Delta robot motion stabilization for flexible packaging of viscous fluid products in a bag", M.Sc.thesis, TU/e, 2021.

[9] H. Groenhuis, "A design tool for electromechanical servo systems", Ph.D. thesis, University of Twente, 1991.

[10] W. Singhose, and L. Pao, "A comparison of input shaping and time-optimal flexible-body control", *Control Engineering Practice*, vol. 5 (4), pp. 459-467, 1997.